Fibroblasts lacking nuclear lamins do not have nuclear blebs or protrusions but nevertheless have frequent nuclear membrane ruptures

Natalie Y. Chen[a], Paul Kim[a], Thomas A. Weston[a], Lovelyn Edillo[a], Yiping Tu[a], Loren G. Fong[a,1,2], and Stephen G. Young[a,b,c,1,2]

[a]Department of Medicine, University of California, Los Angeles, CA 90095; [b]Department of Human Genetics, University of California, Los Angeles, CA 90095; and [c]The Molecular Biology Institute, University of California, Los Angeles, CA 90095

Contributed by Stephen G. Young, August 14, 2018 (sent for review July 23, 2018; reviewed by William T. Dauer and Howard J. Worman)

The nuclear lamina, an intermediate filament meshwork lining the inner nuclear membrane, is formed by the nuclear lamins (lamins A, C, B1, and B2). Defects or deficiencies in individual nuclear lamin proteins have been reported to elicit nuclear blebs (protrusions or outpouchings of the nuclear envelope) and increase susceptibility for nuclear membrane ruptures. It is unclear, however, how a complete absence of nuclear lamins would affect nuclear envelope morphology and nuclear membrane integrity (i.e., whether nuclear membrane blebs or protrusions would occur and, if not, whether cells would be susceptible to nuclear membrane ruptures). To address these issues, we generated mouse embryonic fibroblasts (MEFs) lacking all nuclear lamins. The nuclear lamin-deficient MEFs had irregular nuclear shapes but no nuclear blebs or protrusions. Despite a virtual absence of nuclear blebs, MEFs lacking nuclear lamins had frequent, prolonged, and occasionally nonhealing nuclear membrane ruptures. By transmission electron microscopy, the inner nuclear membrane in nuclear lamin-deficient MEFs have a "wavy" appearance, and there were discrete discontinuities in the inner and outer nuclear membranes. Nuclear membrane ruptures were accompanied by a large increase in DNA damage, as judged by γ-H2AX foci. Mechanical stress increased both nuclear membrane ruptures and DNA damage, whereas minimizing transmission of cytoskeletal forces to the nucleus had the opposite effects.

nuclear lamina | nuclear envelope | nuclear membrane rupture

The nuclear lamina is an intermediate filament meshwork lining the inner nuclear membrane and is composed of A-type and B-type nuclear lamins (1, 2). The nuclear lamina provides structural support for the cell nucleus and interacts with the nuclear chromatin, transcription factors, and proteins of the inner nuclear membrane (1, 2).

For years, the nuclear lamins were thought to play essential roles in the cell nucleus. In particular, B-type lamins were thought to play roles in DNA synthesis (3–5) and in the assembly of the mitotic spindle (6, 7). Recent studies by Jung et al. (8) showed that this is not the case; keratinocytes and fibroblasts proliferate normally and survive in the absence of nuclear lamins. Studies with embryonic stem cells support the idea that nuclear lamin-deficient cells can proliferate and differentiate (9, 10). These newer insights demand a better understanding of the physiologic importance of the nuclear lamina.

One clue into the function of the nuclear lamina is that deficiencies in nuclear lamins or structural defects in nuclear lamins result in nuclear blebs (protrusions or outpouchings of the nuclear envelope) (11–14). Nuclear blebs occur in fibroblasts from patients with Hutchinson–Gilford progeria syndrome (a progeroid syndrome caused by a mutant form of prelamin A) (15), and blebs are common in lamin B1-deficient fibroblasts (16). The mechanisms for nuclear bleb formation are not fully understood, but Funkhouser et al. (11) proposed that separations of nuclear lamin filamentous networks cause nuclear blebs.

Another clue to the function of the nuclear lamina is the observation that defects or deficiencies in nuclear lamins result in nuclear membrane ruptures, leading to intermixing of nucleoplasmic and cytoplasmic contents (17–21) and DNA damage (21, 22). The assumption has been that nuclear membrane ruptures originate from nuclear blebs (19, 22–26).

In the current study, we generated mouse embryonic fibroblasts (MEFs) lacking all nuclear lamins. We wanted to determine whether those cells would manifest nuclear blebs (or protrusions of the chromatin beyond the bounds of the nuclear membranes). We also wanted to determine whether cells lacking nuclear lamins would be susceptible to nuclear membrane ruptures—or whether the absence of nuclear lamin filaments might actually protect from nuclear membrane ruptures.

Results

Nuclear Lamin-Deficient Mouse Embryonic Fibroblasts. We generated $Lmna^{+/+}Lmnb1^{-/-}Lmnb2^{+/+}$ MEFs [lamin B1 knockout (B1KO)], $Lmna^{+/-}Lmnb1^{-/-}Lmnb2^{-/-}$ MEFs [expressing lamin A/C from one allele but no B-type lamins (A1B0)], and $Lmna^{-/-}Lmnb1^{-/-}Lmnb2^{-/-}$ MEFs [triple knockout (TKO)]. TKO MEFs were created by treating $Lmna^{-/-}Lmnb1^{fl/fl}Lmnb2^{fl/fl}$ MEFs (8, 27) with *Cre* adenovirus. TKO MEFs did not express transcripts for prelamin A, lamin C, lamin B1, or lamin B2, as judged by qRT-PCR (Fig. 1*A*). As expected, nuclear lamin proteins were absent from TKO MEFs, as judged by Western blots (Fig. 1*B*) and immunofluorescence microscopy (Fig. 1 *C* and *D*). B1KO MEFs lacked lamin B1 but had normal levels of lamins A, C, and B2. A1B0 MEFs lacked lamins B1 and B2 but had half-normal amounts of lamins A and C (Fig. 1 *B*–*D*).

Significance

Genetic defects in nuclear lamins or reduced expression of nuclear lamins is accompanied by nuclear blebs and an increased susceptibility for nuclear membrane ruptures. Nuclear membrane ruptures are exacerbated by subjecting cells to mechanical forces. Here, we demonstrate that cells lacking nuclear lamins have oblong nuclei, but no nuclear blebs and no protrusions of the chromatin beyond the bounds of the nuclear membranes. Nevertheless, the cells displayed frequent and prolonged nuclear membrane ruptures, associated with DNA damage and occasionally by cell death. Thus, the nuclear lamina is crucial for the integrity of the nuclear membranes and for limiting damage to DNA. We suspect that our observations could be relevant to disease caused by defects or deficiencies in the nuclear lamins.

Author contributions: N.Y.C., L.G.F., and S.G.Y. designed research; N.Y.C., P.K., T.A.W., L.E., and Y.T. performed research; N.Y.C. and P.K. contributed new reagents/analytic tools; N.Y.C. and S.G.Y. analyzed data; and N.Y.C., L.G.F., and S.G.Y. wrote the paper.

Reviewers: W.T.D., University of Michigan; and H.J.W., Columbia University.

The authors declare no conflict of interest.

[1]L.G.F. and S.G.Y. contributed equally to this work.

[2]To whom correspondence may be addressed. Email: lfong@mednet.ucla.edu or sgyoung@mednet.ucla.edu.

This article contains supporting information online at www.pnas.org/lookup/suppl/doi:10.1073/pnas.1812622115/-/DCSupplemental.

Published online September 17, 2018.

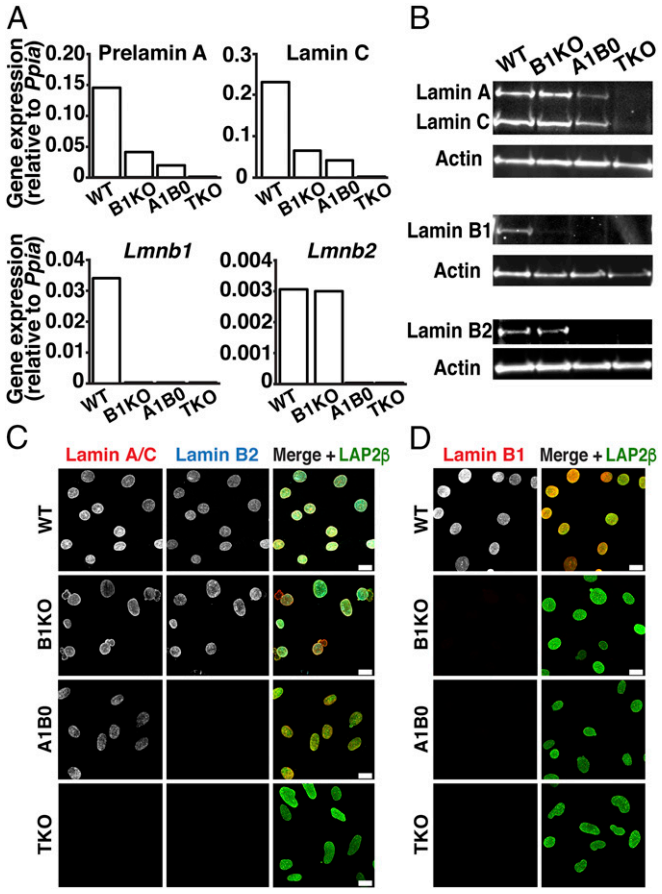

Fig. 1. Mouse embryonic fibroblasts (MEFs) lacking nuclear lamins. (*A*) Transcript levels for prelamin A, lamin C, lamin B1, and lamin B2 in *Lmna*$^{+/+}$*Lmnb1*$^{+/+}$*Lmnb2*$^{+/+}$ [wild-type (WT)], *Lmna*$^{+/+}$*Lmnb1*$^{-/-}$*Lmnb2*$^{+/+}$ [lamin B1 knockout (B1KO)], *Lmna*$^{+/-}$*Lmnb1*$^{-/-}$*Lmnb2*$^{-/-}$ [expressing lamin A/C from one allele but no B-type lamins (A1B0)], and *Lmna*$^{-/-}$*Lmnb1*$^{-/-}$*Lmnb2*$^{-/-}$ [triple-knockout (TKO)] MEFs. Expression was normalized to *Ppia*; mean of two independent experiments. (*B*) Western blots showing nuclear lamin expression in MEFs. Actin was used as a loading control. (*C*) Immunofluorescence microscopy of MEFs with antibodies against lamin A/C (red), lamin B2 (blue), and LAP2β (green). (Scale bars, 20 μm.) (*D*) Immunofluorescence microscopy of MEFs with antibodies against lamin B1 (red) and LAP2β (green). (Scale bars, 20 μm.)

An Absence of Nuclear Blebs in TKO MEFs. Nuclei of WT MEFs were round or oval, and nuclear blebs were very rare (Fig. 2 *A* and *B*). Nuclei from B1KO and A1B0 MEFs were round or oval, but 10.7 ± 3.3% of B1KO MEFs and 16.2 ± 5.3% of A1B0 MEFs had nuclear blebs (Fig. 2 *A* and *B*). Nuclear blebs in TKO MEF nuclei were rare (2.0 ± 1.2%; n = 527 cells), but 84.0 ± 4.1% of nuclei were oblong or irregularly shaped (Fig. 2 *A*, *C*, and *D*). In TKO MEFs, we never observed herniation or protrusion of chromatin beyond the bounds of the nuclear membranes [visualized with the inner nuclear membrane marker LAP2β (lamina-associated polypeptide 2, β isoform)]. Nuclear pore complexes (NPCs) were asymmetrically distributed in TKO MEFs (*SI Appendix*, Fig. S1 *A* and *B*), in keeping with results in an earlier study (9).

By transmission electron microscopy (TEM), both inner and outer nuclear membranes of TKO MEFs were "wavy," whereas only the outer nuclear membrane was wavy in WT MEFs (Fig. 2 *E* and *F* and *SI Appendix*, Fig. S2*A*).

Frequent Nuclear Ruptures in TKO MEFs. To assess susceptibility of TKO MEFs to nuclear membrane ruptures, we expressed an NLS-GFP reporter (green fluorescent protein with a nuclear localization signal) (22) in MEFs and visualized cells by fluorescence microscopy (*SI Appendix*, Fig. S3*A*). In WT MEFs, NLS-GFP was nearly always confined to the nucleus, but the NLS-GFP in TKO MEFs was often present in the cytoplasm, indicating the presence of a nuclear membrane rupture (19, 20, 22). Nuclear membrane ruptures were also rare in wild-type MEFs as they moved across the substrate (Fig. 3*A*, *Top*, and Movie S1). In contrast, nuclear membrane ruptures were frequent in migrating TKO MEFs (Fig. 3*A*, *Bottom*, and Movie S2). In most cases, the ruptures were repaired, and the NLS-GFP returned to the nucleus. Nuclear membrane ruptures often occurred repetitively in the same fibroblast.

To determine the frequency of nuclear membrane ruptures in TKO MEFs, we imaged NLS-GFP–expressing TKO MEFs for 20 h. Numbers of nuclear membrane ruptures and the percentage

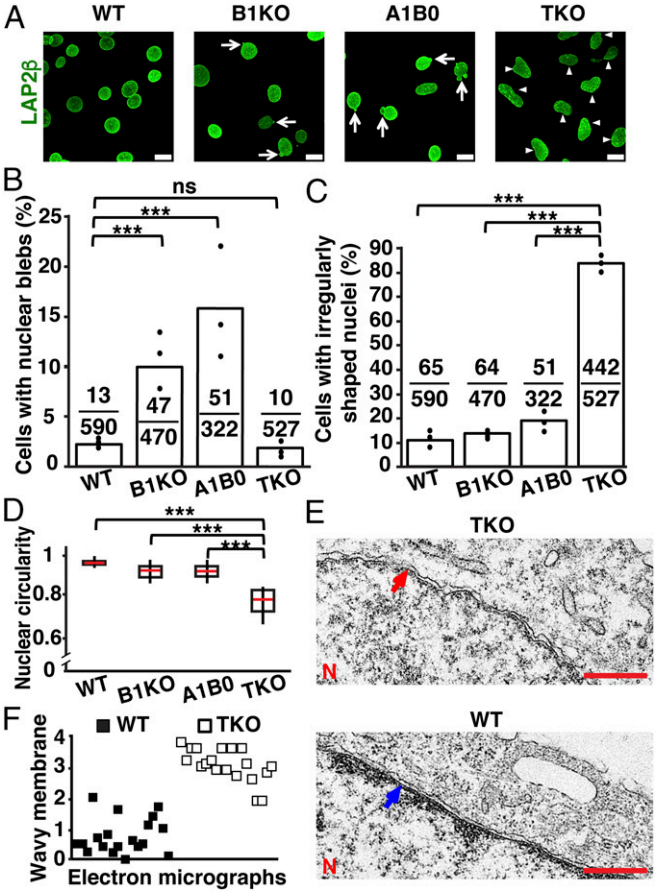

Fig. 2. Morphological abnormalities in WT, B1KO, A1B0, and TKO MEFs. (*A*) Immunofluorescence microscopy of MEFs stained with an antibody against LAP2β (green). The arrows point to nuclear blebs; the arrowheads point to irregularly shaped nuclei. (Scale bars, 20 μm.) (*B*) Percentages of cells with nuclear blebs. The black circles show the averages for three independent experiments; fractions show numbers of cells with blebs divided by the total number of cells examined. ***P < 0.0001 by χ^2 test; ns, nonsignificant, P > 0.05. (*C*) Percentages of cells with irregularly shaped nuclei. The black circles indicate the averages for three independent experiments; fractions show the numbers of cells with irregularly shaped nuclei divided by the total number of cells examined. ***P < 0.0001 by χ^2 test. (*D*) Box plots showing reduced circularity of the nucleus in TKO MEFs. The red line denotes the population median; boxes show 25th and 75th percentiles; and vertical lines show the 10th and 90th percentiles. ***P < 0.0001 by unpaired Student's t test. (*E*) Electron micrographs showing that the inner nuclear membrane in TKO MEFs is wavy (*red* arrow), whereas it is straighter in WT MEFs (blue arrow). N, nuclei. (Scale bar, 500 nm.) (*F*) Scatter plot showing the average "wavy membrane score" for 38 electron micrographs (19 WT and 19 TKO MEFs) by 10 observers blinded to genotype. Each square represents the average score for an image (0 representing the "least wavy" and 4 representing the "most wavy"). WT MEFs (black squares); TKO MEF electron micrographs (white squares).

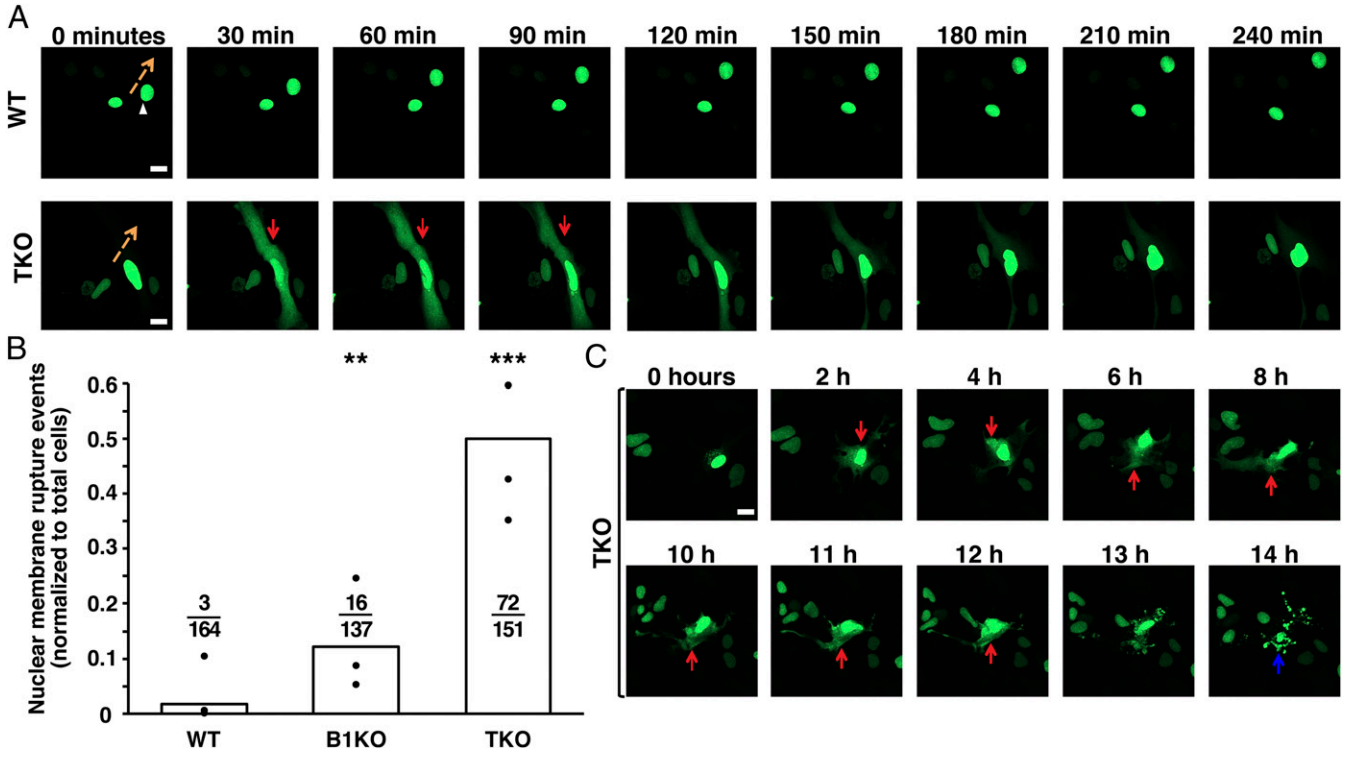

Fig. 3. Nuclear membrane ruptures in TKO MEFs. (*A*) Sequential images of WT and TKO MEFs expressing a green fluorescent protein fused to a nuclear localization signal (NLS-GFP) (green) and imaged by live-cell fluorescence microscopy for 240 min. Images at 30-min intervals are shown. The orange arrows indicate the direction of nuclear movement, and the red arrows point to a nuclear membrane rupture event in a TKO MEF. (*B*) Bar graph showing the number of nuclear membrane ruptures as a percentage of the total number of cells evaluated. The black circles show the averages for three independent experiments. Ratios above each genotype show the total number of nuclear membrane rupture events divided by the total number of cells evaluated. Nuclear membrane ruptures were more frequent in TKO and B1KO MEFs than in WT MEFs. $^{**}P < 0.001$; $^{***}P < 0.0001$ by χ^2 test. (*C*) Sequential images showing a nonhealing nuclear membrane rupture in a TKO MEF (NLS-GFP remains in the cytoplasm) and cell death after 14 h. (Scale bars: *A* and *C*, 20 μm.)

of fibroblasts with nuclear membrane ruptures were higher in TKO MEFs than in WT or B1KO MEFs ($P < 0.0001$) (Fig. 3*B* and *SI Appendix*, Fig. S3*B*). We observed 72 nuclear membrane ruptures in 151 TKO MEFs. Also, nuclear membrane ruptures were more prolonged in TKO MEFs (241 ± 66 min in TKO MEFs vs. 94.4 ± 39 min in B1KO MEFs) (*SI Appendix*, Fig. S3*C*). When TKO MEFs were seeded at high density, nuclear membrane ruptures were observed in migrating cells squeezing between closely packed cells (*SI Appendix*, Fig. S3*D* and Movie S3).

Earlier studies suggested that nuclear membrane ruptures occurred at sites of nuclear blebs (12, 19, 22, 25), but ruptures were common in TKO MEFs despite a virtual absence of blebs. To determine whether nuclear membrane blebs formed before nuclear membrane ruptures, TKO MEFs were imaged at 15-s intervals (*SI Appendix*, Fig. S4*A* and Movies S4–S6). We never observed nuclear blebs or protrusions before nuclear membrane ruptures, suggesting that nuclear blebs are not a prerequisite for nuclear membrane ruptures. Also, we observed no apparent correlation between nuclear membrane ruptures and nuclear blebs in B1KO MEFs (*SI Appendix*, Fig. S4*B*). We identified 16 nuclear membrane ruptures in 137 B1KO MEFs (6.5 ± 1.4%) (Fig. 3*B*), but only 3 of the 16 ruptures occurred in cells harboring a nuclear bleb (*SI Appendix*, Fig. S4 *B* and *C* and Movies S7–S9).

We observed examples of nonhealing nuclear membrane ruptures in TKO MEFs, and those cells invariably died (Fig. 3*C* and Movies S10 and S11), implying that persistent interspersion of cytoplasmic and nucleoplasmic contents is incompatible with cell survival. We suspected that nuclear membrane ruptures in TKO MEFs might lead to DNA damage. Indeed, γ-H2AX foci were far more frequent in TKO MEFs than in WT MEFs (*SI Appendix*, Fig. S5).

TKO and B1KO MEFs harboring nuclear membrane ruptures had gaps and irregularities in the distribution of LAP2β (Fig. 4 *A* and *B* and *SI Appendix*, Fig. S6*A*). In WT MEFs (Fig. 2*A*) and mutant MEFs without ruptures (*SI Appendix*, Fig. S6*B*), LAP2β was homogenously distributed at the nuclear rim. In MEFs with nuclear membrane ruptures, we occasionally observed significant colocalization of NLS-GFP with the ER-resident protein calreticulin, presumably reflecting a ruptured inner nuclear membrane and entry of NLS-GFP into the ER (Fig. 4*C*). More frequently, there was minimal colocalization with calreticulin and NLS-GFP was located throughout the cytoplasm, reflecting ruptures of both inner and outer nuclear membranes (*SI Appendix*, Fig. S6*C*). By TEM, we identified short discontinuities in either the inner or the outer nuclear membranes in TKO MEFs (Fig. 4*D* and *SI Appendix*, Fig. S7), but we never found a gaping hole involving both the inner and outer nuclear membranes.

Disrupting the Cytoskeleton Reduces Nuclear Membrane Ruptures in TKO MEFs. Cytochalasin D reduced the percentage of TKO MEFs with irregularly shaped nuclei (11.3 ± 0.9% vs. 73.2 ± 1.2% in untreated cells) (Fig. 5 *A*, *B*, and *G*), likely by reducing transmission of cytoskeletal forces to the nucleus. Similarly, disrupting the LINC complex with the KASH domain of nesprin 2 (KASH2) (28) reduced the percentage of cells with irregularly shaped nuclei (Fig. 5 *C* and *G*). Neither cytochalasin D nor KASH2 corrected the distribution of NPCs in TKO MEFs (*SI Appendix*, Fig. S1 *C* and *D*), nor did those interventions normalize the wavy inner nuclear membrane phenotype (*SI Appendix*, Fig. S2 *B* and *C*).

We examined the frequency of nuclear membrane ruptures in WT and TKO MEFs under static conditions and with biaxial stretching. Under static conditions, nuclear membrane ruptures were detected in 1.9 ± 0.2% of WT MEFs and 10.7 ± 1.7% of TKO MEFs. When stretched, the frequency of nuclear membrane ruptures was 3.2 ± 1.7% in WT cells vs. 37.3 ± 6.4% in TKO MEFs

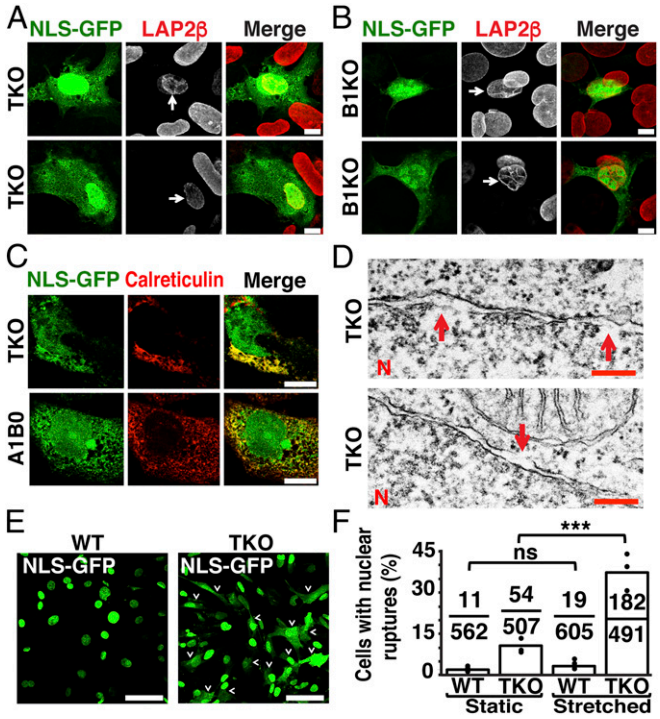

Fig. 4. Increased nuclear membrane ruptures in MEFs lacking nuclear lamins. (*A* and *B*) Immunofluorescence microscopy showing abnormal LAP2β distribution (red) in TKO (*A*) and B1KO (*B*) cells harboring nuclear membrane ruptures (arrows). (Scale bars, 10 μm.) (*C*) Fluorescence microscopy of MEFs with nuclear membrane ruptures (i.e., NLS-GFP in the cytoplasm) and stained with an antibody against calreticulin (ER marker; red). Cytoplasmic NLS-GFP was detected within the ER (yellow) and outside the ER (green). (Scale bars, 10 μm.) (*D*) Electron micrographs showing breaks (red arrows) in the inner (*Top*) and the outer nuclear membrane (*Bottom*) of TKO MEFs. N, nuclei. (Scale bars, 200 nm.) (*E*) Fluorescence microscopy showing larger numbers of nuclear membrane ruptures in TKO MEFs subjected to biaxial stretching. WT and TKO MEFs were subjected to biaxial stretching for 24 h. Nuclear membrane ruptures were frequent, as judged by NLS-GFP (green) in the cytoplasm (arrowheads). (Scale bars, 50 μm.) (*F*) Bar graph showing effects of stretching on nuclear membrane ruptures in WT and TKO MEFs. The black circles indicate frequencies in three independent experiments. Ratios above each genotype show the number of cells with NLS-GFP in the cytoplasm divided by the number of cells scored. ***$P < 0.0005$; ns, nonsignificant, $P > 0.05$ by χ^2 test.

(Fig. 4 *E* and *F*). Cytochalasin D reduced the frequency of nuclear membrane ruptures in TKO MEFs (Fig. 5 *H* and *I*). Under static conditions, 13 ± 7.2% of untreated TKO MEFs had nuclear membrane ruptures vs. 2.8 ± 1.7% in cells treated with cytochalasin D (Movie S12). When TKO MEFs were subjected to biaxial stretching, 43 ± 11.1% of untreated cells had nuclear membrane ruptures vs. 6.8 ± 4.2% in cells treated with cytochalasin D (Fig. 5*I*). Cytochalasin D also reduced the frequency of DNA damage (as judged by γ-H2AX foci), both under static conditions and with stretching ($P < 0.0005$) (Fig. 5 *J*–*L* and *SI Appendix*, Fig. S8).

Partial Rescue of Nuclear Abnormalities in TKO MEFs by Individual Nuclear Lamins. We expressed individual nuclear lamins in TKO MEFs at levels comparable to those in wild-type MEFs (*SI Appendix*, Fig. S9 *A*–*C*). The expression of each nuclear lamin improved the distribution of NPCs, with the NPC distribution mirroring the distribution of the nuclear lamin (*SI Appendix*, Fig. S1 *E*–*G*). Lamin A expression, but not lamin B1 or B2 expression, reversed the wavy inner nuclear membrane phenotype (*SI Appendix*, Fig. S2 *D*–*F*). Expression of either lamin A or lamin B1 reduced the percentage of cells with irregularly shaped nuclei ($P < 0.0001$) but simultaneously elicited nuclear blebs (Fig. 5 *D*, *E*, and *G* and *SI Appendix*, Fig. S9*G*). Lamin A in transfected TKO MEFs was distributed in a "honeycomb" pattern, in contrast to the even distribution pattern of lamin A in WT MEFs (*SI Appendix*, Fig. S9*D*) and the even distribution of lamin B1 in transfected TKO MEFs (*SI Appendix*, Fig. S9*E*). Lamin B2 was unevenly distributed in lamin B2-expressing TKO MEFs, and lamin B2 did not correct the irregular nuclear shape phenotype (Fig. 5 *F* and *G* and *SI Appendix*, Fig. S9*F*). Lamin B1 expression reduced the frequency of nuclear membrane ruptures, whereas lamin B2 expression did not (Fig. 5*H* and Movies S13 and S14). Unexpectedly, lamin A expression in TKO MEFs increased the frequency of nuclear membrane ruptures (Fig. 5*H* and Movie S15). The duration of ruptures in lamin A-expressing TKO MEFs was shorter than in nontransfected TKO MEFs (*SI Appendix*, Fig. S9*H*), but the shorter duration of ruptures was not accompanied by reduced DNA damage (*SI Appendix*, Fig. S9*I*).

Discussion

We examined nuclear membrane morphology and nuclear membrane ruptures in fibroblasts lacking all nuclear lamins (TKO MEFs) and gleaned five insights. First, nuclei in TKO MEFs are oblong and irregularly shaped but nuclear blebs are virtually absent. Cytochalasin D normalized nuclear shape, implying that cytoskeletal forces cause the abnormal nuclear shape. Second, the absence of nuclear lamins in TKO MEFs was accompanied by discrete discontinuities in either the inner or outer nuclear membranes but no gaping holes, as judged by TEM. A hallmark of TKO MEFs is a wavy inner nuclear membrane. The expression of lamin A largely normalized that phenotype, while the effects of the B-type lamins were far less impressive. Third, despite a virtual absence of nuclear blebs in TKO MEFs, nuclear membrane ruptures were frequent. These ruptures were prolonged and accompanied by DNA damage. In most cases, the nuclear membrane ruptures eventually healed, but in some cells the ruptures persisted, resulting in cell death. Fourth, nuclear membrane ruptures and the accompanying DNA damage were exaggerated by mechanical stretching and minimized by interventions that reduce force transmission to the nucleus (e.g., actin depolymerization, disrupting the LINC complex). These observations support earlier reports that external forces on the nucleus promote nuclear membrane ruptures (19, 22–26, 29). Fifth, transfection of TKO MEFs with individual nuclear lamin proteins did not abolish nuclear membrane ruptures, implying that a combination of several nuclear lamins is required for maintaining nuclear membrane integrity.

Earlier studies showed that mutations or deficiencies in nuclear lamin proteins can elicit nuclear blebs and nuclear membrane ruptures (11–14), leading to the assumption that nuclear membrane ruptures originate from weak segments of the nuclear envelope (i.e., blebs). However, we found that nuclear membrane ruptures in TKO MEFs are frequent despite an absence of blebs. Our data from live-cell imaging at 15-s intervals provided no indication that blebs or protrusions precede nuclear membrane ruptures, although we cannot exclude the possibility that the blebs are so evanescent that they simply cannot be visualized with this approach. Also, in B1KO MEFs, only a few of the nuclear membrane ruptures occurred in cells harboring nuclear blebs. Also, the expression of lamin B1 in TKO MEFs increased the frequency of nuclear blebs while reducing the frequency of nuclear membrane ruptures.

Expressing lamin A in TKO MEFs increased the frequency of nuclear membrane ruptures, whereas lamin B1 reduced the frequency of ruptures. In the case of lamin B1, we suspect that the association of its farnesyl lipid anchor with the inner nuclear membrane serves to immobilize lamin B1 filaments and thereby preserve the integrity of the inner nuclear membrane. Mature lamin A lacks a lipid anchor; consequently, lamin A filaments have greater mobility and might even pierce the nuclear membranes (particularly when the membranes are not buffered by a layer of lamin B1 filaments). We believe that this scenario is plausible. In keratinocytes lacking nuclear lamins, keratin filaments can be visualized in the cell nucleus, raising the possibility that those filaments may have pierced the nuclear membranes (8).

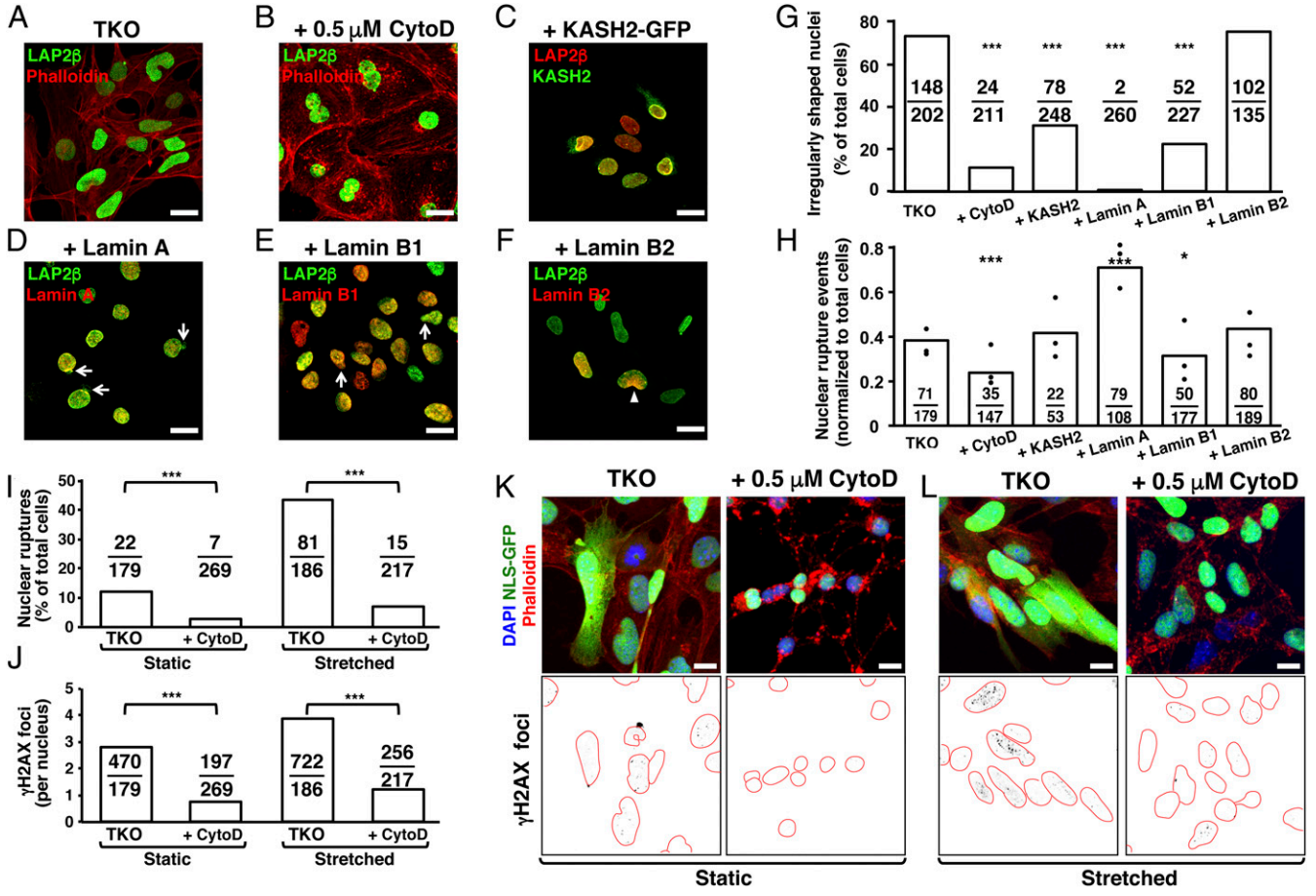

Fig. 5. Impact of actin depolymerization, disrupting the LINC complex, and nuclear lamin expression on nuclear morphology, nuclear membrane ruptures, and DNA damage in TKO MEFs. (*A–F*) Fluorescence microscopy images of TKO MEFs treated with 0.5 μM cytochalasin D (to disrupt the cytoskeleton); TKO MEFs expressing the KASH domain of nesprin 2 (KASH2-EGFP; to disrupt the LINC complex); and expressing human prelamin A (pTRIPZ-hu-prelamin A), human lamin B1 (pTRIPZ-*LMNB1*), or human lamin B2 (pTRIPZ-*LMNB2*). Cells were stained to visualize LAP2β, actin (with phalloidin), KASH2, lamin A, lamin B1, or lamin B2. Expression of lamin A and lamin B1 elicited nuclear blebs (arrows). In most cells, lamin B2 was not expressed uniformly in the nucleus (arrowhead). (Scale bars, 20 μm.) (*G*) Percentage of TKO MEFs with irregularly shaped nuclei. The ratios show the number of cells with irregularly shaped nuclei divided by the total number of cells examined. Treatment groups vs. control: $***P < 0.0001$ by χ^2 test. (*H*) Number of nuclear membrane ruptures in TKO MEFs. The results were analyzed as described in *G*. Treatment groups vs. control: $*P < 0.01$, $***P < 0.0001$ by χ^2 test. (*I*) Bar graph showing that cytochalasin D reduces the frequency of nuclear membrane ruptures in static and stretched TKO MEFs. The results were analyzed as described in *G*. $***P < 0.0001$ by χ^2 test. (*J*) Bar graph showing that cytochalasin D reduces γ-H2AX foci in static and stretched TKO MEFs. The results were analyzed as described in *G*. $***P < 0.0005$ by Student's *t* test. (*K* and *L*) Fluorescence microscopy images showing that cytochalasin D reduces γ-H2AX foci in static (*K*) and stretched (*L*) TKO MEFs. Panels below images show γ-H2AX foci (black) inside nuclei (outlined in red). (Scale bars: *K* and *L*, 10 μm.)

By TEM, we observed short discontinuities in the inner nuclear membrane and the outer nuclear membrane, but despite exhaustive efforts found no gaping holes involving both inner and outer nuclear membranes. However, it is conceivable that we simply overlooked large breaches, given that only ∼15% of the cells have nuclear membrane ruptures at any given time. Also, we imaged only a small portion of the cell nucleus; our TEM sections were 65 nm thick, while the nucleus is several micrometers thick.

Our studies underscored functional differences between lamin B1 and lamin B2. Both lamin B1 and lamin B2 are uniformly distributed along the nuclear rim in wild-type cells (13, 14, 30). When those proteins are expressed in TKO MEFs, lamin B1 is uniformly distributed along the nuclear rim, whereas in many cells lamin B2 is distributed in an inhomogeneous fashion. Also, in contrast to lamin B1, lamin B2 had no capacity to elicit nuclear blebs in TKO MEFs or to correct the wavy inner nuclear membrane phenotype. The distinct properties of the two B-type lamins are consistent with our earlier findings. In lamin B1-deficient neurons, the distribution of lamin B2 is inhomogeneous, whereas lamin B1 is distributed normally in lamin B2-deficient neurons (13). Also, the farnesyl lipid anchor is crucial for lamin B1 stability and function, whereas lamin B2's farnesyl lipid tail is dispensable (30).

By immunofluorescence microscopy, we observed two intriguing findings. The first is that occasional TKO MEFs with nuclear membrane ruptures displayed substantial colocalization of NLS-GFP and calreticulin. In those cells, we suspect that an inner nuclear membrane rupture allowed NLS-GFP to enter the perinuclear space and then enter the ER lumen (where calreticulin resides). The second observation is that TKO MEFs with nuclear membrane ruptures invariably had gaps and irregularities in the distribution of LAP2β, whereas LAP2β was evenly distributed in cells without nuclear membrane ruptures. We do not know whether the profoundly abnormal distribution of LAP2β preceded the nuclear membrane ruptures or was a consequence of the ruptures. We cannot completely exclude the possibility that the gaps in LAP2β distribution reflected gaping holes in the nuclear membranes, but our TEM studies provided no support for that possibility.

In summary, our studies demonstrate that an absence of nuclear lamins leads to frequent and prolonged nuclear membrane ruptures and DNA damage. Ultimately, we suspect that our findings will prove relevant to disease phenotypes, for example

the progressive loss of cortical neurons accompanying deficiencies of lamin B1 or lamin B2 (13, 14, 30, 31).

Materials and Methods

Cell Culture. To generate TKO MEFs (*Lmna*$^{-/-}$*Lmnb1*$^{-/-}$*Lmnb2*$^{-/-}$), we treated *Lmna*$^{-/-}$*Lmnb1*$^{fl/fl}$*Lmnb2*$^{fl/fl}$ MEFs as described previously (8, 27) with *Cre* adenovirus. To generate fluorescently labeled cell lines with the nuclear rupture reporter NLS-GFP (22), we transduced cells with lentivirus by UCLA's Vector Core Facility.

RNA Studies. qRT-PCR (qPCR) studies were performed with the primers listed in *SI Appendix*, Table S1.

Western Blots. Urea-soluble protein extracts from cells were prepared (32), and Western blots were performed with the antibodies listed in *SI Appendix*, Table S2.

Immunofluorescence Microscopy. Cells on coverslips were fixed with 4% paraformaldehyde in PBS or ice-cold methanol followed by one dip in acetone and permeabilized with 0.2% Triton. The cells were then processed for confocal immunofluorescence microscopy (27) using antibodies listed in *SI Appendix*, Table S2.

Nuclear Shape Analysis. To quantify percentages of cells with nuclear blebs and cells with irregularly shaped nuclei, we stained MEFs with an antibody against LAP2β (*SI Appendix*, Table S2). Fluorescence images of randomly selected nuclei were acquired at 20× on a Zeiss LSM700 laser-scanning microscope. Nuclei of WT, B1KO, A1B0, and TKO MEFs were scored as normal, having one or more nuclear blebs, or irregularly shaped (deviating from a spherical shape, oblong) by an independent observer blinded to genotype. At least 300 cells were scored per group.

Electron Microscopy. Cells were prepared by fixing and scraping monolayers of cells or by en face embedding of adherent cells grown on Thermanox (Ted Pella) coverslips. Details are included in *SI Appendix, SI Materials and Methods*.

Live-Cell Imaging. Live-cell imaging was performed with 35-mm glass-bottom microwell Petri dishes (MatTek) or six-well plates containing 2-mm glass wells (MatTek) on a Zeiss LSM 800 confocal microscope with a Plan Apochromat 10×/0.45 or a Plan Apochromat 20×/0.80 objective at 37 °C with 5% CO_2 maintained by TempModule S1 (Zeiss) and CO_2 Module S1 (Zeiss). *Z* stacks were acquired from fluorescence and transmission channels in sequential order at indicated time steps.

Cell Stretching. Stretching MEFs on polydimethylsiloxane (PDMS) membranes was performed as described (33). Cells were seeded on flexible PDMS membranes (1 mm thick). The membranes were stretched 5 mm at 0.5 Hz for 24 h. To test the effects of cytochalasin D on nuclear membrane ruptures, the membranes were stretched 2 mm at 0.5 Hz for 2 h.

Treatment of Cells with Cytochalasin D. MEFs were treated with 0.5 μM cytochalasin D (Tocris) for 1 h before live-cell imaging or fixation for immunofluorescence microscopy. For cell-stretching experiments, MEFs were treated with 0.5 μM cytochalasin D for 3 h before being stretched 2 mm at 0.5 Hz for 3 h.

Expression Vectors for Nuclear Lamins and KASH2. pTRIPZ-Prelamin A was generated with a human prelamin A cDNA (#SC101048; Origene) (33). pTRIPZ-*LMNB1* and pTRIPZ-*LMNB2* were generated by introducing a human lamin B1 cDNA (#SC116661; Origene) or a human lamin B2 cDNA (#SC106163; Origene) into the pTRIPZ vector with Infusion Cloning (Clontech). The EGFP-KASH2 sequence was amplified from pEGFP-C1-KASH2 (34) subcloned into the pLenti6/v5-DEST plasmid (Thermo Fisher).

Statistical Analyses. Statistical analyses were performed with GraphPad QuickCalcs (https://www.graphpad.com/). Differences in nuclear morphologies (blebs, irregularly shaped nuclei) and nuclear membrane rupture frequency were analyzed with a χ^2 test. Differences in nuclear circularity and numbers of γ-H2AX foci were assessed by two-tailed Student's *t* test.

See *SI Appendix, SI Materials and Methods* for more details on the methods we used.

ACKNOWLEDGMENTS. We thank Dr. Dino Di Carlo (UCLA) for the use of the membrane cleaning device. We thank Dr. Jan Lammerding for sharing the NLS-GFP plasmid and for observations that inspired us to embark on this project. Virus production and transduction were performed by the Integrated Molecular Technologies Core/UCLA Vector Core, which is supported by Center for Ulcer Research and Education/P30 DK041301. This work was supported by National Institutes of Health Grant HL126551 (to S.G.Y.) and Grant AG047192 (to L.G.F.), National Institutes of Health Ruth L. Kirschstein National Research Service Award T32GM065823 (to N.Y.C.), and a Whitcome Fellowship award from UCLA's Molecular Biology Institute.

1. Worman HJ, Fong LG, Muchir A, Young SG (2009) Laminopathies and the long strange trip from basic cell biology to therapy. *J Clin Invest* 119:1825–1836.
2. Burke B, Stewart CL (2013) The nuclear lamins: Flexibility in function. *Nat Rev Mol Cell Biol* 14:13–24.
3. Moir RD, Montag-Lowy M, Goldman RD (1994) Dynamic properties of nuclear lamins: Lamin B is associated with sites of DNA replication. *J Cell Biol* 125:1201–1212.
4. Moir RD, et al. (2000) Review: The dynamics of the nuclear lamins during the cell cycle—relationship between structure and function. *J Struct Biol* 129:324–334.
5. Ellis DJ, Jenkins H, Whitfield WG, Hutchison CJ (1997) GST-lamin fusion proteins act as dominant negative mutants in *Xenopus* egg extract and reveal the function of the lamina in DNA replication. *J Cell Sci* 110:2507–2518.
6. Tsai MY, et al. (2006) A mitotic lamin B matrix induced by RanGTP required for spindle assembly. *Science* 311:1887–1893.
7. Harborth J, Elbashir SM, Bechert K, Tuschl T, Weber K (2001) Identification of essential genes in cultured mammalian cells using small interfering RNAs. *J Cell Sci* 114:4557–4565.
8. Jung HJ, et al. (2014) An absence of nuclear lamins in keratinocytes leads to ichthyosis, defective epidermal barrier function, and intrusion of nuclear membranes and endoplasmic reticulum into the nuclear chromatin. *Mol Cell Biol* 34:4534–4544.
9. Guo Y, Zheng Y (2015) Lamins position the nuclear pores and centrosomes by modulating dynein. *Mol Biol Cell* 26:3379–3389.
10. Kim Y, Zheng X, Zheng Y (2013) Proliferation and differentiation of mouse embryonic stem cells lacking all lamins. *Cell Res* 23:1420–1423.
11. Funkhouser CM, et al. (2013) Mechanical model of blebbing in nuclear lamin meshworks. *Proc Natl Acad Sci USA* 110:3248–3253.
12. Hatch E, Hetzer M (2014) Breaching the nuclear envelope in development and disease. *J Cell Biol* 205:133–141.
13. Coffinier C, et al. (2011) Deficiencies in lamin B1 and lamin B2 cause neurodevelopmental defects and distinct nuclear shape abnormalities in neurons. *Mol Biol Cell* 22:4683–4693.
14. Coffinier C, et al. (2010) Abnormal development of the cerebral cortex and cerebellum in the setting of lamin B2 deficiency. *Proc Natl Acad Sci USA* 107:5076–5081.
15. Eriksson M, et al. (2003) Recurrent de novo point mutations in lamin A cause Hutchinson–Gilford progeria syndrome. *Nature* 423:293–298.
16. Vergnes L, Péterfy M, Bergo MO, Young SG, Reue K (2004) Lamin B1 is required for mouse development and nuclear integrity. *Proc Natl Acad Sci USA* 101:10428–10433.
17. Hatch EM (2018) Nuclear envelope rupture: Little holes, big openings. *Curr Opin Cell Biol* 52:66–72.
18. De Vos WH, et al. (2011) Repetitive disruptions of the nuclear envelope invoke temporary loss of cellular compartmentalization in laminopathies. *Hum Mol Genet* 20:4175–4186.
19. Vargas JD, Hatch EM, Anderson DJ, Hetzer MW (2012) Transient nuclear envelope rupturing during interphase in human cancer cells. *Nucleus* 3:88–100.
20. Hatch EM, Fischer AH, Deerinck TJ, Hetzer MW (2013) Catastrophic nuclear envelope collapse in cancer cell micronuclei. *Cell* 154:47–60.
21. Raab M, et al. (2016) ESCRT III repairs nuclear envelope ruptures during cell migration to limit DNA damage and cell death. *Science* 352:359–362.
22. Denais CM, et al. (2016) Nuclear envelope rupture and repair during cancer cell migration. *Science* 352:353–358.
23. Lammerding J, Wolf K (2016) Nuclear envelope rupture: Actin fibers are putting the squeeze on the nucleus. *J Cell Biol* 215:5–8.
24. Isermann P, Lammerding J (2017) Consequences of a tight squeeze: Nuclear envelope rupture and repair. *Nucleus* 8:268–274.
25. Hatch EM, Hetzer MW (2016) Nuclear envelope rupture is induced by actin-based nucleus confinement. *J Cell Biol* 215:27–36.
26. de Noronha CMC, et al. (2001) Dynamic disruptions in nuclear envelope architecture and integrity induced by HIV-1 Vpr. *Science* 294:1105–1108.
27. Yang SH, et al. (2011) An absence of both lamin B1 and lamin B2 in keratinocytes has no effect on cell proliferation or the development of skin and hair. *Hum Mol Genet* 20:3537–3544.
28. Razafsky D, Hodzic D (2014) Temporal and tissue-specific disruption of LINC complexes in vivo. *Genesis* 52:359–365.
29. McGregor AL, Hsia CR, Lammerding J (2016) Squish and squeeze-the nucleus as a physical barrier during migration in confined environments. *Curr Opin Cell Biol* 40:32–40.
30. Jung HJ, et al. (2013) Farnesylation of lamin B1 is important for retention of nuclear chromatin during neuronal migration. *Proc Natl Acad Sci USA* 110:E1923–E1932.
31. Young SG, Jung HJ, Coffinier C, Fong LG (2012) Understanding the roles of nuclear A- and B-type lamins in brain development. *J Biol Chem* 287:16103–16110.
32. Fong LG, et al. (2004) Heterozygosity for Lmna deficiency eliminates the progeria-like phenotypes in Zmpste24-deficient mice. *Proc Natl Acad Sci USA* 101:18111–18116.
33. Kim P, et al. Disrupting the LINC complex in smooth muscle cells ameliorates aortic disease in a mouse model of Hutchinson–Gilford progeria syndrome. *Sci Transl Med*, in press.
34. Stewart-Hutchinson PJ, Hale CM, Wirtz D, Hodzic D (2008) Structural requirements for the assembly of LINC complexes and their function in cellular mechanical stiffness. *Exp Cell Res* 314:1892–1905.